Int J Clin Exp Med 2019;12(3):2209-2215
www.ijcem.com /ISSN:1940-5901/IJCEM0085852

Original Article

Microvasculature femoral head cartilage and subchondral bone in patients with ankylosing spondylitis

Lisheng Wu[1*], Yi Sun[2*], Jinhua Zi[1], Bing Zhu[1,3], Jun Chen[4], Cunhua Zhang[1], Shijie Xu[1], Daozhang Cai[5], Wanli Gao[1]

[1]Department of Orthopedics, Linyi People's Hospital, Linyi, Shandong Province, China; [2]Department of Preventive Medicine, School of Basic Medical Sciences, Shandong Medical College, Shandong Province, China; [3]Graduate School, Tai Shan Medical University, Taian, Shandong Province, China; [4]Department of Bone and Joint Injury Rehabilitation, Linyi Rehabilitation Hospital, Linyi, Shandong Province, China; [5]Department of Orthopedics, Third Affiliated Hospital of Southern Medical University, Guangzhou, China. [*]Equal contributors.

Received September 22, 2018; Accepted February 13, 2019; Epub March 15, 2019; Published March 30, 2019

Abstract: Objective: To investigate the possible pathological mechanism of hip osteotropia in patients with ankylosing spondylitis (AS) through the quantification of microvascular density in femoral head cartilage and subchondral bone. Methods: The experimental group comprised samples of femoral head tissue obtained from 7 patients with AS. The control group comprised samples of femoral head tissue obtained from 11 patients with osteoarthritis (OA) and 9 patients with rheumatoid arthritis (RA). The expression levels of vascular endothelial growth factor (VEGF), CD56+, and CD68+ were measured. A semi-quantitative assessment was performed using Leica Qwin high-definition image analysis. Results: The results showed an increased density of the microvasculature at the bone-cartilage interface on the femoral head in patients with AS, compared with patients with OA ($P < 0.01$) or RA ($P < 0.05$). The presence of CD68+ multinuclear cells at the osteochondral junction was interpreted as evidence of bone absorption. CD68+ expression was significantly increased in patients with AS, compared with patients with OA ($P < 0.05$) or RA ($P < 0.01$). In AS patients with a femoral head denuded of cartilage, increased levels of bony destruction were observed (8.04 ± 1.43 vs. 5.14 ± 1.62; $P < 0.01$). Conclusion: In patients with AS, the bone-cartilage interface and subchondral bone showed signs of inflammation, including an increased area of the microvasculature. Such phenomena may contribute to the progression of hip osteotropia.

Keywords: Ankylosing spondylitis, immunohistochemistry, vascular endothelial growth factor

Introduction

Ankylosing spondylitis (AS) is a common, chronic, highly hereditary, immune-mediated arthritis that affects the spine and sacroiliac joints, as well as surrounding joints and extra-articular tissues, including the eyes, intestines, and skin. This is the prototype of Spa, a group of rheumatic diseases with clinical, genetic, and radiologic characteristics. Over time, bone formation occurs, leading to bony fusion (ankylosis) and osteophyte formation in the sacroiliac joint. This process is characterized by osteophyte growth and associated with progressive chronic back pain, decreased activity, and possibly hypnosis. Connective tissue may eventually bridge the adjacent vertebrae, resulting in reduced spinal mobility and disability [1]. In contrast to reports on patients with rheumatoid arthritis (RA), studies have shown that synovium is not the main site of inflammation in patients with AS [2]. However, the mechanisms underlying its clinical and pathological manifestations remain to be elucidated [3]. In recent years, experts have achieved a broad consensus with regard to genetic risk factors and aspects of the immune response involved in the initial stages of disease. Although the available data are relatively scarce, abnormal bone formation is considered to be the most significant pathogenic factor associated with disease progression [4].

Vascular endothelial growth factor (VEGF) is an effective angiogenic vasoactive molecule that enhances vascular permeability and acts as a

mitogen in the presence of endothelial cells [5]. It has been suggested that high serum levels of VEGF correlate with levels of disease activity in patients with spondylarthropathies [6]. Serum levels of VEGF are increased in AS patients [7] and correlate with disease activity [6]. The predictive value of serum VEGF levels in interpreting radiologic progression has also recently been confirmed [8]. For example, increased vascularity is a prominent feature of AS synovitis [9].

Few studies have investigated the potential role of serum VEGF levels in the management of AS or VEGF expression levels in the cartilage of AS patients. In this study, VEGF levels in femoral head tissue from patients with AS were determined by immunohistochemistry and compared with levels in samples from control patients with OA or RA. The expression of CD56+ on osteoblasts and the expression of CD68+ on osteoclasts were measured to explore the relationship between the density of the microvasculature and hip osteotropia in patients with AS.

Materials and methods

Study patients

Femoral head specimens were collected from patients seen at the Department of Orthopedics, Linyi People's Hospital during the period June 2015 to January 2017. Seven AS patients (5 male, 2 female), aged 25-72 years (mean 53.2 years), who had been diagnosed according to New York standards revised in 1984, were included in the study. Eleven OA patients (7 male, 4 female), aged 55-78 years (mean 61.4 years) and 9 patients with RA (5 male, 4 female), aged 34-75 years (mean 55.8 years), served as the control group. Patient ages were similar across all groups. Except for the 2 AS patients, all the subjects included in the study had cartilage remaining on the femoral head, which had cartilaginous as well as noncartilaginous areas. All patients, or their parents, approved their participation in the study. Ethical approval was obtained from the Ethics Committee of Linyi People's Hospital (Lin No. 201503).

Sample collection

After the specimen was obtained, it was immediately fixed with 4% paraformaldehyde and stored at 4°C for 2-4 h. The specimen was then transferred into a solution of 30% sucrose in phosphate-buffered saline (PBS) and stored at 4°C overnight. The femoral head covered with cartilage and/or without cartilage, was divided into paraffin sections respectively. The sections were cut to a thickness of 10 μm and adhered to slides coated with adhesive and stored at 80°C.

A Leica Qwin high-definition image analysis system (Leica, Germany) was used to analyze the femoral head surface. Rabbit anti-human polyclonal antibody VEGF (Ph.D., BA0407); mouse anti-human monoclonal antibody CD56+ (MAB0256) CD68+ (MAB0041), and SP (kit KIT-9709) were purchased from Fujian Mai Xin Company. Anti-tartrate acid phosphatase was purchased from the Sigma-Aldrich Company (USA). An ELF-97 Immunohistochemical Kit was purchased from Invitrogen (USA).

Immunohistochemistry

In order to ensure optimal adhesion of the tissue to be used for immunostaining, sections with a thickness of 4-6 μm were cut, then baked for 20 minutes at 60°C. Paraffin sections were dewaxed and hydrated, then washed in PBS for 5 min, and this was repeated 3 times. After the addition of a 3% methanol hydrogen peroxide solution, the sections were stored at room temperature for 10 min, then they were washed with PBS for 5 min, 3 times. The sections were then submerged in a 0.01 M sodium citrate buffer (pH 6.0) and stored at 95°C. Then paraffin sections were heated for 10-15 min and washed in PBS for 5 min, and this was repeated 3 times. The sections were blocked with normal goat serum. The slides were stored at room temperature for 20 min. After the absorption of excess liquid, 50 μL anti-I (anti-rabbit anti-human VEGF polyclonal antibody; monoclonal antibodies CD56 and CD68) was added. Sections were stored for 1 h at room temperature, then washed with PBS for 5 min 3 times. Fifty μL anti-II (biotinylated goat anti-rabbit IgG) was added. The sections were stored for 1 h at room temperature, then they were washed with PBS for 5 min × 3 times. After DAB was added for 5-10 min, the sections were evaluated under a microscope to determine the degree of staining. The slides were washed with PBS for 10 min, then they were stained with hematoxylin and dehydrated. The transparent sections were dried. The results were observed under a microscope. In the section × 200 times view backup, LeicaQwin high definition graphic analyzer gray value detection with

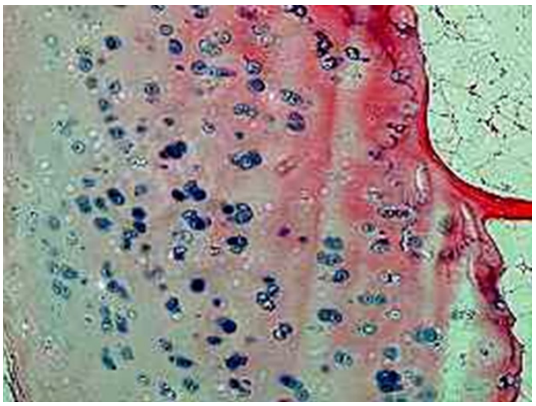

Figure 1. HE staining of cartilaginous (× 200) femoral head tissue in AS. Cartilage cells are distributed throughout the cartilaginous areas.

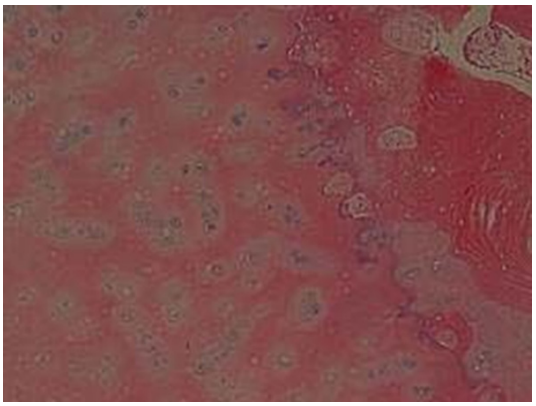

Figure 2. HE staining of non-cartilaginous (× 200) femoral head tissue in AS. Few chondrocytes are observed in the non-cartilaginous area.

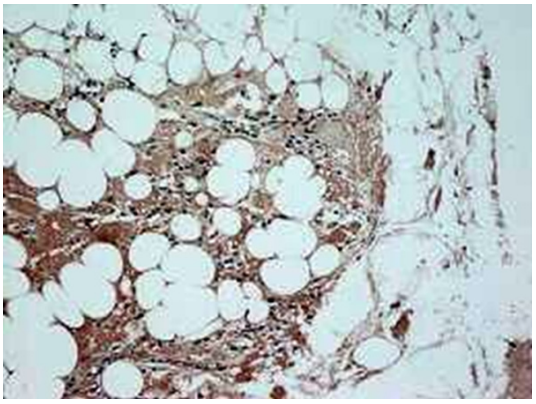

Figure 3. VEGF expression in cartilaginous (× 200) femoral head tissue in AS. Strong VEGF staining can be seen in the subchondral bone.

or without cartilage covering the area of positive cell aggregates count. Areas of bone destruction were defined as areas of subchondral bone or cartilage with ≥5 CD68+ multinucleate osteoclasts. Because CD68+ is not specific for the expression of osteoclasts, we used tartrate resistant acid phosphatase (TRAP) staining to detect osteoclast [10] at 37°C after 10 min of incubation, and the application of osteoclast phosphatase substrate ELF-97 produced fluorescent products [11]. The microvascular density of the endothelial cells was assessed by the immunohistochemistry of the antibody against VEGF. Density of the microvasculature was expressed as the mean value of each high-powered field.

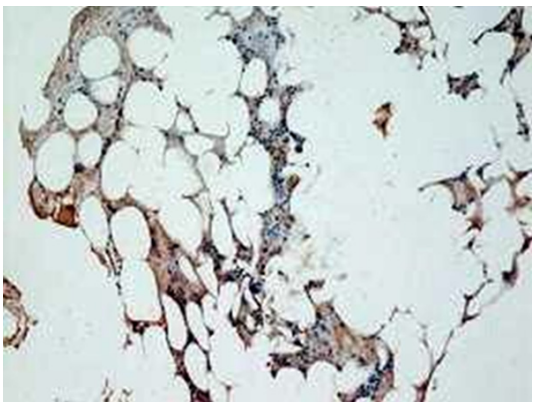

Figure 4. VEGF expression in non-cartilaginous (× 200) femoral head tissue in AS. Limited VEGF staining can be seen in the subchondral bone.

Statistical analysis

Statistical analyses were performed with SPSS 12.0 software. Measurement data are expressed as $\bar{x} \pm S$. All variables were verified using a Kolmogorov-Smirnov test to conform to the normal distribution, and Bartlett's method was used to verify the homogeneity of variance. Two independent sample mean *t* tests were used to compare the experimental group and the control group. The groups were compared using an analysis of variance, using $\alpha = 0.05$ or 0.01. $P < 0.05$ indicates that the discrepancy had statistical significance. $P < 0.01$ indicates that the discrepancy had remarkable significance.

Results

Hematoxylin and eosin (HE) staining of the femoral head sections from patients with AS showed that cartilage cells were evenly distributed throughout the cartilaginous areas (**Figure 1**). Few chondrocytes were observed in the

Table 1. Numbers ($\bar{x}$ ± S) of positive cell aggregates on the surface of the femoral head and in the non-cartilaginous area on the femoral head

Groups	n	Count of positive cell aggregation		
		VEGF	CD56+	CD68+
Cartilaginous area				
AS	5	12.97 ± 4.31	26.63 ± 7.84	5.14 ± 1.62
OA	11	4.43 ± 1.32**	29.25 ± 6.7	11.51 ± 0.93*
RA	9	7.42 ± 3.35$^{\#}$	25.72 ± 5.93	0.87 ± 0.60$^{\#\#}$
Non-cartilaginous area				
AS	7	11.92 ± 6.48*	42.50 ± 9.42**	8.04 ± 1.43**
OA	11	6.60 ± 5.15	31.87 ± 7.34	1.70 ± 1.02
RA	9	12.73 ± 6.63	27.59 ± 6.71	1.51 ± 0.87

AS: Ankylosing spondylitis, OA: Osteoarthritis, RA: Rheumatoid arthritis. Cartilaginous area: AS: OA, $^{**}P < 0.01$, $^{*}P < 0.05$; AS: RA, $^{\#\#}P < 0.01$, $^{\#}P < 0.05$; AS Cartilaginous area: No cartilaginous area, $^{**}P < 0.01$, $^{*}P < 0.05$.

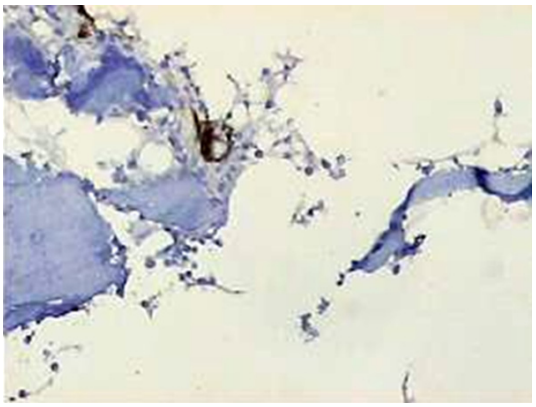

Figure 5. Femoral head CD56+ expression at the bone-cartilage interface in AS, cartilaginous area (× 200). CD56+ cells are scattered throughout the subchondral bone.

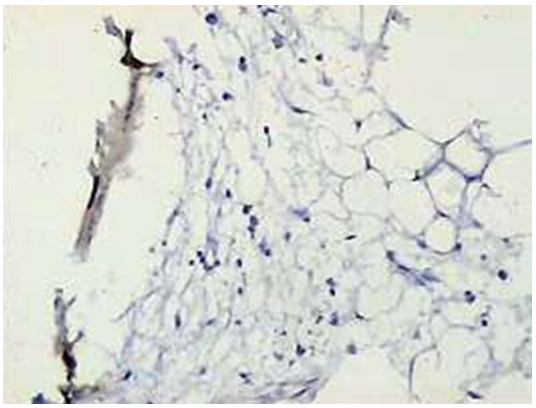

Figure 6. Femoral head CD56+ expression at the bone-cartilage interface in AS, non-cartilaginous area (× 200). Abundant CD56+ cells are observed throughout the subchondral bone.

non-cartilaginous area (**Figure 2**). There are VEGF in AS of bone and cartilage and subchondral bone interface (**Figures 3**, **4**). The density of the microvasculature in the cartilaginous areas of the bone-cartilage interface on the femoral head was increased in patients with AS, compared with patients with OA (12.97 + 4.31 vs. 4.43 + 1.32; $P < 0.01$) or RA (12.97 + 4.31 vs. 7.42 + 3.35; $P < 0.05$) (**Table 1**).

The samples obtained from the femoral heads of the areas free of cartilage were compared with those obtained from the femoral heads with cartilaginous areas. The results showed a slight decrease in density of the microvasculature (**Figure 5**; **Table 1**), but this trend did not reach statistical significance ($P > 0.05$). Among patients with AS, femoral heads lacking cartilage showed increased osteoblast density (26.63 + 7.84 vs. 42.50 + 9.42, $P < 0.01$) (**Figure 6**; **Table 1**). The osteoblast density was similar between patients with OA and patients with RA.

In patients with AS, increased numbers of cells displaying osteoclast morphology (CD68+ multinucleated cells) were observed in the areas of bone resorption at the osteochondral junction on the femoral head surfaces with cartilaginous areas (**Figure 7**). Areas of bone erosion on the femoral head surface were increased in patients with AS, compared with patients with OA (5.14 + 1.62 vs. 1.51 + 0.93; $P < 0.05$) or RA (5.14 + 1.62 vs. 0.87 + 0.60; $P < 0.01$) (**Table 1**). Compared with the cartilaginous femoral head surfaces in patients with AS, those lacking cartilage showed significantly increased levels of bone erosion (8.04 + 1.43 vs. 5.14 + 1.62; $P < 0.01$) (**Figure 8**; **Table 1**). In patients with RA, noncartilaginous femoral head surfaces showed higher levels of subchondral bone erosions, compared with cartilaginous femoral head surfaces (**Table 1**). However, this difference was not statistically significant ($P > 0.05$).

Discussion

Analysis of the femoral head surface in patients with AS showed increased density of the micro-

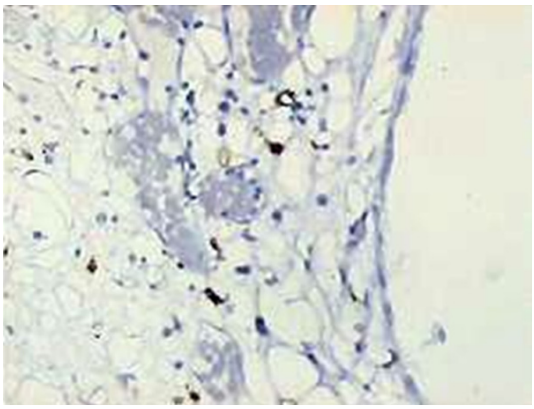

Figure 7. Femoral head CD68+ expression at the subchondral interface in AS, cartilaginous area (× 200). Abundant CD68+ cells are observed throughout the subchondral bone.

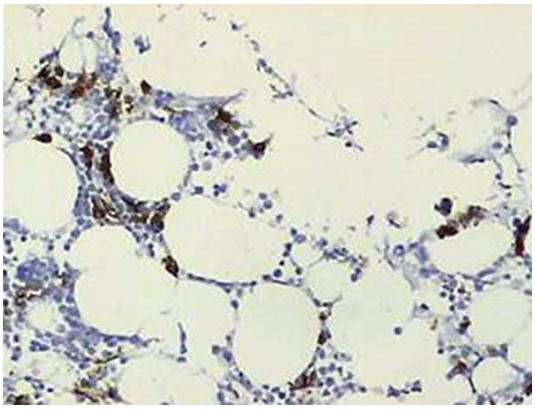

Figure 8. Femoral head CD68+ expression at the subchondral interface in AS, non-cartilaginous area (× 200). CD68+ cells are scattered throughout the subchondral bone.

vasculature at the bone-cartilage interface and in the subchondral bone. These findings indicate that angiogenesis is partly related to local immunology and pathology. The loss of cartilage mononuclear cells is representative of late-stage inflammation in AS. In this study, osteoblast activation was accompanied by enhanced vascularization. Neovascularization is essential for inflammation as well as the formation of bone [12]. Studies have confirmed that VEGF has osteogenic effects that accelerate the healing of fractures [13-17]. Ossification must be associated with angiogenesis. During the early stage of ossification, VEGF-mediated angiogenesis indicates the initiation of ossification [18]. Higher serum levels of VEGF may contribute to the pathogenesis of AS through Wnt signaling [19]. In AS, VEGF in synovial tissues may participate in the differentiation of fibroblasts into osteoclasts [20]. One recent study showed that serum VEGF levels were significantly associated with inflammation and the immune response in AS [21].

The results presented above indicate increased numbers of osteoclasts in cartilage-covered portions of the femoral head in patients with AS, compared with patients with RA or OA. This finding suggests that the osteoclast-mediated absorption of bone may be facilitated by an environment that stimulates inflammation and thus induces the expression of hydrolase. Tissue factors release matrix collagenase, alter the extracellular matrix, and mediate the destruction of bone and cartilage [22]. High levels of osteoclast activity and an increased density of the microvasculature usher in the late stage of joint involvement, resulting in bony ankylosis. Clinical studies have shown that osteoclasts are the main effectors of bone destruction. Furthermore, the ossification and stiffness of normal ligaments and synovium are essential to the progression of osteoarthritis [23]. However, the conditions for the differentiation of osteoclast precursors remain unclear, hindering efforts at prevention and treatment of the disease. As an important inflammatory initiation factor, tumor necrosis factor-α (TNF-α) plays an important role in the inflammation and differentiation of tumor cells [24].

Conclusion

The osteochondral interface and subchondral bone are the main sites of inflammation in AS. The results presented above suggest that the microvasculature plays an important role in inducing inflammation and hip osteotropia in patients with AS. Additional studies will be necessary to elucidate the underlying mechanism.

Acknowledgements

None of the authors has a financial relationship with a commercial entity that has an interest in the subject of this manuscript. This work was supported by the Unite Special Project of the Natural Science Foundation of Shandong Province (#ZR2015HL032) and the development projects of Shandong Province Science and Technology of Traditional Chinese Medicine (#2013ZDZK155).

Disclosure of conflict of interest

None.

Address correspondence to: Wanli Gao, Department of Orthopedics, Linyi People's Hospital, No. 27, Jiefang Road, Lanshan District, Linyi, Shandong Province, China. Tel: +86 539 8038767, +86159-53988537; E-mail: tsyxyzb@163.com; gaowanli1977@163.com

References

[1] Lories RJ, Luyten FP, de Vlam K. Progress in spondylarthritis. Mechanisms of new bone formation in spondyloarthritis. Arthritis Res Ther 2009; 11: 221.

[2] Maksymowych WP. Ankylosing spondylitis--at the interface of bone and cartilage. J Rheumatol 2000; 27: 2295-2301.

[3] McGonagle D, Gibbon W, O'Connor P, Green M, Pease C, Emery P. Characteristic magnetic resonance imaging entheseal changes of knee synovitis in spondylarthropathy. Arthritis Rheum 1998; 41: 694-700.

[4] de Koning A, Schoones JW, van der Heijde D, van Gaalen FA. Pathophysiology of axial spondyloarthritis: consensus and controversies. Eur J Clin Invest 2018; 48: e12913.

[5] Jain RK. Molecular regulation of vessel maturation. Nat Med 2003; 9: 685-693.

[6] Drouart M, Saas P, Billot M, Cedoz JP, Tiberghien P, Wendling D, Toussirot E. High serum vascular endothelial growth factor correlates with disease activity of spondylarthropathies. Clin Exp Immunol 2003; 132: 158-162.

[7] Goldberger C, Dulak J, Duftner C, Weidinger F, Falkenbach A, Schirmer M. Vascular endothelial growth factor (VEGF) in ankylosing spondylitis--a pilot study. Wien Med Wochenschr 2002; 152: 223-225.

[8] Poddubnyy D, Conrad K, Haibel H, Syrbe U, Appel H, Braun J, Rudwaleit M, Sieper J. Elevated serum level of the vascular endothelial growth factor predicts radiographic spinal progression in patients with axial spondyloarthritis. Ann Rheum Dis 2014; 73: 2137-2143.

[9] Kidd BL, Moore K, Walters MT, Smith JL, Cawley MI. Immunohistological features of synovitis in ankylosing spondylitis: a comparison with rheumatoid arthritis. Ann Rheum Dis 1989; 48: 92-98.

[10] Rozenszajn L, Marshak G, Efrati P. Acid phosphatase activity in normal human blood and bone marrow cells as demonstrated by the azo dye method. Acta Haematol 1963; 30: 310-316.

[11] Filgueira L. Fluorescence-based staining for tartrate-resistant acidic phosphatase (TRAP) in osteoclasts combined with other fluorescent dyes and protocols. J Histochem Cytochem 2004; 52: 411-414.

[12] Deckers MM, Karperien M, van der Bent C, Yamashita T, Papapoulos SE, Lowik CW. Expression of vascular endothelial growth factors and their receptors during osteoblast differentiation. Endocrinology 2000; 141: 1667-1674.

[13] Li R, Nauth A, Li C, Qamirani E, Atesok K, Schemitsch EH. Expression of VEGF gene isoforms in a rat segmental bone defect model treated with EPCs. J Orthop Trauma 2012; 26: 689-692.

[14] Li R, Li CH, Nauth A, McKee MD, Schemitsch EH. Effect of human vascular endothelial growth factor gene transfer on endogenous vascular endothelial growth factor mRNA expression in a rat fibroblast and osteoblast culture model. J Orthop Trauma 2010; 24: 547-551.

[15] Zhang Z, Zhang Y, Zhou Z, Shi H, Qiu X, Xiong J, Chen Y. BDNF regulates the expression and secretion of VEGF from osteoblasts via the TrkB/ERK1/2 signaling pathway during fracture healing. Mol Med Rep 2017; 15: 1362-1367.

[16] Song N, Zhao Z, Ma X, Sun X, Ma J, Li F, Sun L, Lv J. Naringin promotes fracture healing through stimulation of angiogenesis by regulating the VEGF/VEGFR-2 signaling pathway in osteoporotic rats. Chem Biol Interact 2017; 261: 11-17.

[17] Liao SS, Guan K, Cui FZ, Shi SS, Sun TS. Lumbar spinal fusion with a mineralized collagen matrix and rhBMP-2 in a rabbit model. Spine (Phila Pa 1976) 2003; 28: 1954-1960.

[18] Won YW, Lee M, Kim HA, Bull DA, Kim SW. Post-translational regulated and hypoxia-responsible VEGF plasmid for efficient secretion. J Control Release 2012; 160: 525-531.

[19] Solmaz D, Uslu S, Kozaci D, Karaca N, Bulbul H, Tarhan EF, Ozmen M, Can G, Akar S. Evaluation of periostin and factors associated with new bone formation in ankylosing spondylitis: periostin may be associated with the wnt pathway. Int J Rheum Dis 2018; 21: 502-509.

[20] Liu KG, He QH, Tan JW, Liao GJ. Expression of TNF-alpha, VEGF, and MMP-3 mRNAs in synovial tissues and their roles in fibroblast-mediated osteogenesis in ankylosing spondylitis. Genet Mol Res 2015; 14: 6852-6858.

[21] Wang M, Zhou X, Zhang H, Liu R, Xu N. Associations of the VEGF level, VEGF rs2010963 G/C gene polymorphism and ankylosing spondylitis risk in a chinese han population. Immunol Lett 2016; 179: 56-60.

[22] Olofsson B, Jeltsch M, Eriksson U, Alitalo K. Current biology of VEGF-B and VEGF-C. Curr Opin Biotechnol 1999; 10: 528-535.

[23] Briolay A, Lencel P, Bessueille L, Caverzasio J, Buchet R, Magne D. Autocrine stimulation of osteoblast activity by Wnt5a in response to TNF-alpha in human mesenchymal stem cells. Biochem Biophys Res Commun 2013; 430: 1072-1077.

[24] Scudiero I, Zotti T, Ferravante A, Vessichelli M, Reale C, Masone MC, Leonardi A, Vito P, Stilo R. Tumor necrosis factor (TNF) receptor-associated factor 7 is required for TNFalpha-induced Jun NH2-terminal kinase activation and promotes cell death by regulating polyubiquitination and lysosomal degradation of c-FLIP protein. J Biol Chem 2012; 287: 6053-6061.